IEEE 802.11ax: Joint Effects of Power Control and IQ Imbalance Mitigation Schemes on the Performance of OFDM Uplink Multi-User MIMO

Roger Pierre Fabris Hoefel
Electrical Engineering Department
Federal University of Rio Grande do Sul (UFRGS)
Porto Alegre, RS, Brazil
roger.hoefel@ufrgs.br

***Abstract*—The 802.11ax Specification Framework delivered by the IEEE High Efficiency WLANs (HEW) Task Group (TG) in early 2016 has specified the uplink multi-user multiple-input multiple-output (UL MU-MIMO) as a key medium access control (MAC) and physical layer (PHY) technique to improve the uplink network throughout in ultra-dense networks loaded with small form factor devices. In this paper, we first show that the phase noise (PN) hardware impairment does not degrade the 802.11ax UL MU-MIMO PHY performance even with differences on the received power among the clients. In the following, we show that the effects of in-phase and quadrature (IQ) imbalance on the UL MU-MIMO PHY performance can be catastrophic, especially when it is used high-cardinality modulation schemes without uplink power control. Finally, we show that a joint implementation of an uplink power control scheme and a time-domain IQ mitigation algorithm can mitigate the dramatic effects on the 802.11ax UL MU-MIMO PHY performance due to IQ imbalance and phase noise hardware impairments in channels where the average power received per client at the access point presents a significant standard deviation.**

Keywords—802.11ax; Uplink Multi-User MIMO; Phase Noise; IQ Imbalance; Power Control, Asynchronous Uplink Channel.

I. INTRODUCTION

The TG 802.11ax has included multi-user (MU) transmissions in the 11ax Specification Framework Document (SFD) [1]. Uplink multi-user multiple-input multiple-output (UL MU-MIMO) scheme is a fundamental joint medium access control (MAC) and physical layer (PHY) protocol to improve the network throughput in ultra-dense wireless local area networks (WLANs) in usage cases where the networks are loaded with small form devices that are only capable of transmitting 1-2 spatial streams (SS) [2]. The 802.11ax draft 1.0 [3] was not approved in the group letter ballot that was carried out from December 2016 to January 2017. Therefore, the TG 802.11ax has started to work on resolutions of the remarks submitted on draft D1.0.

In this paper, we analyze and propose schemes for the IEEE 802.11ax UL MU-MIMO PHY in order to counterbalance the effects of phase noise (PN), in-phase and quadrature (IQ) imbalance as well as differences on the average received power and time arrival among the clients. The remaining of this paper has the following layout: Section II describes the analytical models used to simulate the PN and IQ imbalance hardware impairments. Section III describes an uplink power control scheme suitable for uplink multi-user transmission in WLANs. Section IV summarizes the main characteristics of an IEEE 802.11ax PHY simulator. Section V presents a set of simulation results carefully designed to analyze the joint effects of phase noise, IQ imbalance, power control and asynchronous UL channel on the performance of 802.11ax UL MU-MIMO PHY. Section VI contains our final conclusions.

Most of the open literature on the effects of hardware impairments [4] and power control [5-6] on UL MU-MIMO IEEE 802.11ax PHY has been published in TGax meetings. For the best of our knowledge, we have not seen any peer-review paper that focus extensively on the IQ imbalance mitigation and uplink power control for 802.11ax UL MU-MIMO PHY, as we have developed in this paper.

II. PHASE NOISE AND IQ IMBALANCE

A. Phase Noise

The phase noise (PN) hardware impairment for frequencies below 6 GHz, according with the TGax 802.11ax document entitled "*11ax Evaluation Methodology*" [7, pp. 7], is modeled by the following power spectral density (PSD):

$$\mathrm{PSD(f)} = \mathrm{PSD(0)} \cdot \frac{1+(f/f_z)^2}{1+(f/f_p)^2} \quad \left[\frac{dBc}{Hz}\right], \tag{1}$$

where the pole and zero frequencies are given by $f_p = 250\ kHz$ and $f_z = 7905.7\ kHz$, respectively. The PSD at direct current (DC) is specified as -100 dBc/Hz, resulting in $\mathrm{PSD}(\infty) = -130\ \mathrm{dBc/Hz}$. The PN impairment must be modeled at both transmitter and receiver.

Figure 1 shows analytical and simulation results for the PN PSD noise in dBc/Hz as function of the baseband frequency in Hz, where a passband bandwidth (BW) of 80 MHz is assumed.

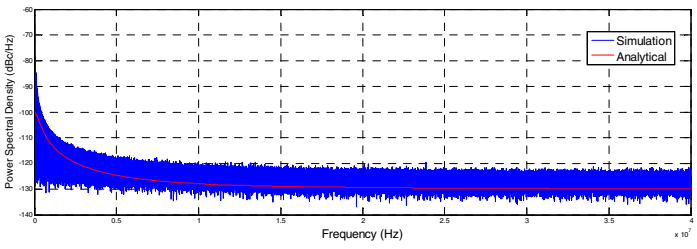

Figure 1. Phase noise power spectral density in dBc/Hz.

978-1-5090-5935-5/17/$31.00 ©2017 IEEE

B. In-Phase and Quadrature Imbalance

The direction-conversion radio-frequency (RF) analog front-end architecture introduces mismatches between the in-phase (I) and quadrature (Q) components. The IQ imbalance can be modeled by the gain error I_a and phase mismatch I_p between the in-phase and quadrature components [8-9]. The IQ imbalance is assumed being constant among all subcarriers. The amplitude impairment can be modeled as follows:

$$y_a = y_{a,re} + jy_{a,im} = y_{re} + j\left(10^{-\frac{I_{a,dB}}{20}} \cdot y_{im}\right), \quad (2)$$

where $y = y_{re} + jy_{im}$ denotes the symbols without amplitude mismatching.

The signal with amplitude and phase imbalance is given by

$$y_{a\&p} = y_{a,re} + j10^{-\frac{I_{a,dB}}{20}}\left[cos(I_p) \cdot y_{a,im} - sin(I_p) \cdot y_{a,re}\right]. \quad (3)$$

The Application Note [10] reports that state-of-art IQ modulators have single side band (SSB) suppression higher than –40 dBc, that corresponds to a gain imbalance of 0.1875 dB and phase imbalance of 0.3º. A SSB suppression of -30 dBc is achievable if the RF analog front-end has a gain imbalance of 0.5 dB and phase imbalance of 1º [10]. In this paper, we assume that the same IQ imbalance is inserted at both transmitter and receiver.

III. Power Control for 802.11ax UL MU-MIMO

There are two classes of devices that support transmission/reception of high-efficiency (HE) trigger based physical layer protocol data units (PPDU): *(i) High Tier Class A devices* (absolute power efficiency of ± 3 dB; received signal strength indication, RSSI, measurement of ± 2 dB); *(ii) Low Tier Class B devices* (absolute power efficiency of ± 9 dB; RSSI measurement of ± 5 dB) [5-6]. Therefore, the maximum difference in power is 10 dB and 28 dB for two devices that belong to Class A and Class B, respectively.

The TG 802.11ax has proposed the following uplink power control (UL-PC) scheme [6]:

1. The access point (AP) transmits a *Trigger Message* that transports the AP transmit power in dBm and the target RSSI in dBm for each STA scheduled for UL MU transmission.
2. Each STA sets in an independent way its transmit power according with the following equation:

$$Tx_{pwr}^{STA}(dBm) = PL_{DL}(dB) + Target_{RSSI}(dBm), \quad (4)$$

   where $PL_{DL}(dB)$ denotes the downlink (DL) path loss estimated by each STA, using the AP transmit power transported in the *Trigger Message* and the measured RSSI.
3. Each station (STA) signals its headroom in the uplink in order that the AP could know the available power for each STA to select the modulation and code scheme (MCS) that optimize the system performance.

In this paper, we propose using a moving average finite impulsive response (FIR) filter with N_{FIR} taps to estimate the downlink RSSI, which is necessary to calculate the path loss used in (4). The input to the FIR filter is the first moment of the RSSI. This random variable is estimated using all pilots transmitted in the legacy-long training field (L-LTF) of the *Trigger Message*. Notice that in a real world implementation it is also necessary to design a dynamic mechanism to reset the filter inputs that exceed a pre-determined time period to avoid estimating the path loss with outdated values.

IV. IEEE 802.11ax Simulator

In this paper, the IEEE 802.11ax UL MU-MIMO PHY system performance is evaluated using a simulator that we have been developing and validating, whose main characteristics are shown in Tab. 1 [11].

Tab. II shows the IEEE 802.11ac/ax MCS analyzed in this paper.

In this paper, we implement an interference cancellation minimum mean squared error (IC-MMSE) MU-MIMO detector [12]. This MU-MIMO detector has more receive antennas than the total number of SS transmitted by all STAs and, consequently, there are spatial degrees of freedom that are only used to improve the cancellation of the multi-user interference.

TABLE I. Basic parameters and characteristics of the IEEE 802.11ax simulator.

Parameter	Value	Parameter	Value
Carrier Frequency	5.25 GHz	MCS	0-9
Bandwidth	20 MHz, 40 MHz, 80 MHz	Number of Spatial Streams	1 to 8
GI Length	800 ns	Synchronization	Auto-Correlation
Modulation	BPSK, QPSK, 16-QAM, 64-QAM, 256-QAM	MIMO Channel Estimation	Least Squares (LS) [13, pp. 98]
Binary Convolutional Code (BCC)	Code rate: r=1/2, r=2/3, r=3/4, r=5/6	Channel Decoder	Hard and Soft-Decision Viterbi Decoding

TABLE II. MCS investigated in this paper. The shown PHY data rates assume a guard-interval (GI) of 800 ns and a BW of 80 MHz.

MCS	Mod	BCC Code Rate	# SSs/ # STAs	Data Rate per STA/ Total Data Rate
0	BPSK	1/2	1/6	29.3/175.8 Mbps
3	16-QAM	1/2	1/6	117/702 Mbps

In the following, we shall show outcomes for TGac B and D channels. The TGac B channel models intra-room and room-to-room residential channels with a maximum excess delay of 390 ns and root mean square (rms) delay spread of 80 ns [13, pp.39, 57]. This channel is lightly frequency selective with spatial correlation at both transmitter and receiver. The TGac D model is spatial-correlated and highly frequency selective fading channel, which is normally used to simulate typical office environments. It has a maximum excess delay of 390 ns and rms delay spread of 50 ns [13, pp. 39, 58]. The UL MU-MIMO channel defined as $[n_t,n_r,K,n_{ss}]$ has the following characteristics: *(i)* each STA has an equal number of n_t transmit antennas; *(ii)* the AP has n_r receive antennas; *(iii)* the channel is loaded with K STAS; *(iv)* each STA transmits an equal number of n_{ss} SS.

In the sequel, the difference on the average power received at the AP among the STAs is denoted by ΔP, e.g., $\Delta P = x$ dB means that half of the clients are x dB weaker than the other half [4]. The simulation results for the packet error rate (PER) shown in this paper refer to the weaker STAs in order to analyze the worst-case performance.

V. Performance Analysis

A. Phase Noise

Figure 2 shows the effects of PN hardware impairment on the medium access control protocol data unit (MPDU) PER as function of signal-to-noise ratio (SNR) in dB for MCS3 (16-QAM). The results shown on the left-corner assume the TGac B [1,8,6,1] channel, while those ones on the right-corner refer to the TGac D [1,8,6,1] channel. It is shown results for $\mathrm{PSD}(0) = -100\ \mathrm{dBc/Hz}$ and for a more aggressive PN impairment with $\mathrm{PSD}(0) = -85\ \mathrm{dBc/Hz}$, resulting in $\mathrm{PSD}(\infty) = -115\ \mathrm{dBc/Hz}$. In this figure, the UL-PC scheme is not implemented. We have concluded that the 11ax UL MU-MIMO transceivers are highly insensitive with relation to (w.r.t.) PN impairments even with received power differences among the clients. Notice that the uplink multi-user interference is the predominant factor on the system performance when the MU MMSE detector is implemented over UL MU-MIMO [1,8,6,1] TGac B and D channels. In the remaining of this paper, we simulate the PN hardware impairment using the parameters reported in Section II.

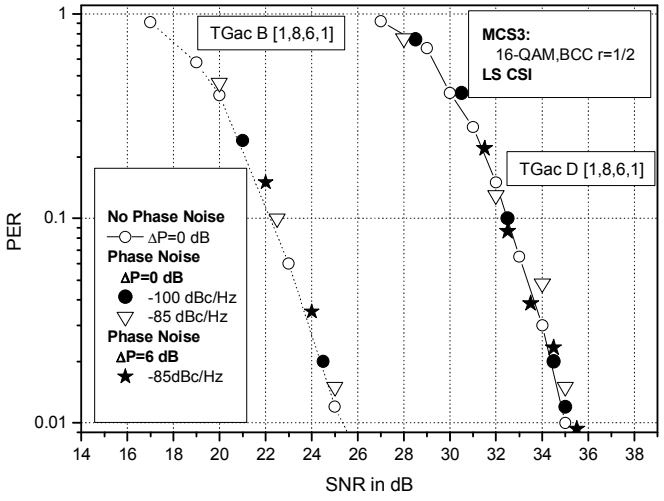

Figure 2. Effects of phase noise on the PER: MCS3 (16-QAM); [1,8,6,1] TGac B and D channels; BW=80 MHz; MU-MMSE receiver with least square (LS) channel state information (CSI), MPDU payload of 1500 bytes; soft-decision Viterbi decoding.

B. IQ Imbalance

Figure 3 allows investigating the joint effects of IQ imbalance, receive power differences among the clients and UL-PC on the performance of 802.11ax UL MU-MIMO PHY over the TGac D [1,8,6,1] channel. We have implemented a moving average FIR filter with order 10 to estimate the RSSI at each STA, which is necessary to implement the PC scheme described in Section III.

Figure 3a (MCS0, BPSK) shows that the proposed UL-PC scheme can mitigate the joint effects of IQ imbalance (SSB suppression of -40 dBc) and differences on the received power (as high as 18 dB). Fig. 3b (MCS3, 16-QAM) shows that the IQ imbalance impairment impinges a power loss of 7 dB for a typical PER of 1%. Notice that Fig. 3a shows that the IQ imbalance does not degrade the system performance for MCS0 when the received power is the same for all STAs. However, Fig. 3b shows a power loss of 7 dB for MCS3 due to the IQ impairment even when the received power is the same for all STAs. It is interesting to observe that a PER higher than 10% occurs for MCS3 when the UL-PC scheme is not implemented in a system with SSB suppression of -40 dBc and power difference between the stronger and weaker clients of 6 dB. Finally, we can see that the proposed UL-PC control scheme can mitigate the effects of power differences among the clients, although the performance loss is still overmuch high (i.e., ~7 dB) due to the IQ imbalance hardware impairment.

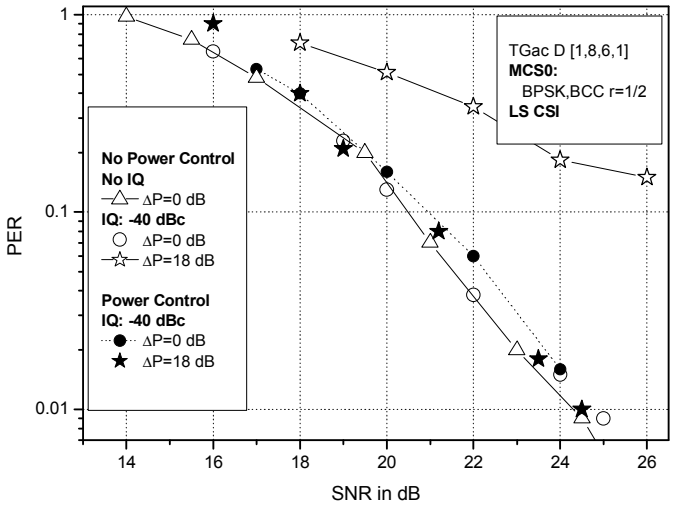

Figure 3a. MCS 0 (BPSK, BCC with code rate ½).

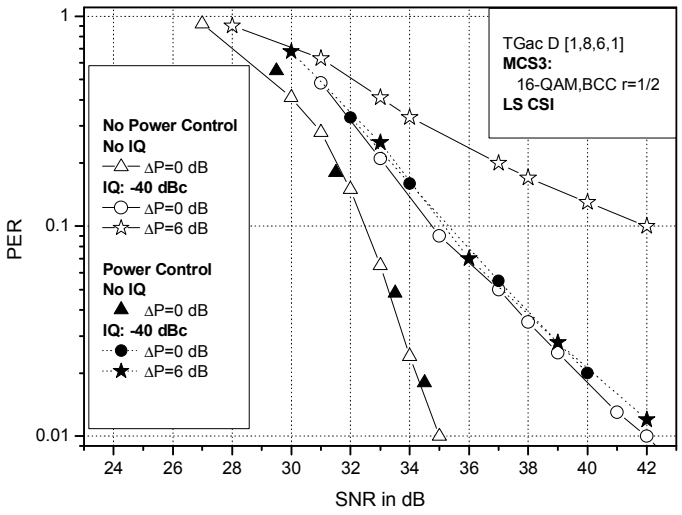

Figure 3b. MCS 3 (16-QAM, BCC with code rate ½).

Figure 3. Effects of IQ imbalance (with SSB suppression of -40 dBc) and power control on the PER: TGac D [1,8,6,1] channel; BW=80 MHz; MU-MMSE receiver with LS CSI, MPDU payload of 1500 bytes; soft-decision Viterbi decoding.

C. IQ Imbalance Mitigation

The earlier results have shown that it is imperative to implement algorithms to mitigate the IQ imbalance in the UL MU-MIMO 802.11ax PHY.

The IEEE 802.11ax legacy preamble contains the legacy-long training field (L-LTF) that has *2* repetitions of a long symbol

plus an extended cyclic prefix $CP_{L\text{-}LTF}$. The extended CP implemented in the L-LTF allows more robustness to the channel delay spread since the L-LTF is used to perform channel estimation and tuning the gross carrier frequency offset (CFO) estimated at the L-STF [11]. Assuming a BW of 80 MHz, then the length of each L-LTF $P_{L\text{-}LTF}$ and the length of the extended cyclic prefix $CP_{L\text{-}LTF}$ have 256 and 128 samples, respectively [13]. The short and long CP used in control and data orthogonal frequency division multiplexing (OFDM) symbols of IEEE 802.11ac/ax frames have 32 (400 ns) and 64 samples (800 ns), respectively, for a BW of 80 MHz.

In this paper, we estimate the IQ amplitude mismatch using a moving average (MA) FIR filter with 10 taps. The input of the FIR filter is given by (5) (as proposed in [9] for IEEE 802.11a/g without using a MA FIR filter), where the $r_I[\mathrm{k}]$ *and* $r_Q[\mathrm{k}]$ denote the in-phase and quadrature components, respectively, of the L-LTF transported in each 802.11ax frame; L represents the number of samples of the L-LTF. Notice that the implemented time domain amplitude imbalance estimation scheme also collects the power received in all n_r received antennas.

$$I_{a,est} = \sqrt{\frac{\sum_{i=1}^{n_r}\sum_{k=1}^{L}\left|\mathrm{r}_Q^{(i)}[\mathrm{k}]\right|^2}{\sum_{i=1}^{n_r}\sum_{k=1}^{L}\left|\mathrm{r}_I^{(i)}[\mathrm{k}]\right|^2}}. \quad (5)$$

The IQ phase imbalance can be estimated by calculating the normalized cross-correlation between the in-phase and quadrature components of the received signal, i.e.,

$$\rho = \frac{\sum_{i=1}^{n_r}\sum_{k=1}^{L}\mathrm{r}_I^{(i)}[\mathrm{k}]\cdot\left(\frac{1}{I_{a,est}}\mathrm{r}_Q^{(i)}[\mathrm{k}]\right)}{\sum_{i=1}^{n_r}\sum_{k=1}^{L}\left|\mathrm{r}_I^{(i)}[\mathrm{k}]\right|^2}. \quad (6)$$

Using the IQ imbalance model given by (3), then (6) can be rewritten as follows:

$$\rho = \frac{\sum_{i=1}^{n_r}\sum_{k=1}^{L}\mathrm{r}_I^{(i)}[k]\cdot\left(\frac{I_a}{I_{a,est}}\left[cos(I_p)\mathrm{r}_Q^{(i)}[\mathrm{k}]-sin(I_p)\mathrm{r}_I^{(i)}[k]\right]\right)}{\sum_{i=1}^{n_r}\sum_{k=1}^{L}\left|r_{I,i}[\mathrm{k}]\right|^2}, \quad (7)$$

which can be approximated, assuming that $I_a = I_{a,est}$, by

$$\rho \approx -sin(I_p). \quad (8)$$

Notice that:

$$cos(I_p) = \sqrt{1-sin^2(I_p)} \approx \sqrt{1-\rho^2}. \quad (9)$$

The amplitude imbalance for the *k*th subcarrier (SC) of the *i*th antenna is corrected as follows:

$$w^{(i)}[\mathrm{k}] = w_I^{(i)}[\mathrm{k}] + w_Q^{(i)}[\mathrm{k}] = \mathrm{r}_I^{(i)}[\mathrm{k}] + j\frac{1}{I_{a,est}}\mathrm{r}_I^{(Q)}[\mathrm{k}]. \quad (10)$$

Finally, the signal with mitigation of both amplitude and phase imbalance for the *k*th SC of the *i*th antenna is given by

$$z^{(i)}[\mathrm{k}] = w_I^{(i)}[\mathrm{k}] + j\frac{1}{\sqrt{1+\rho^2}}\left\{w_Q^{(i)}[\mathrm{k}] - \rho\cdot w_I^{(i)}[\mathrm{k}]\right\}. \quad (11)$$

In this paper, the normalized cross-correlation coefficient (see 6) is used as input of a MA FIR filter to denoise the estimation of (8) and (9). The algorithm to estimate the IQ imbalance at the transmitter (i.e., the STAs in the UL MU-MIMO) uses the L-LTF field transmitted in the *Trigger Frame (TF)*, while the scheme to estimate the IQ imbalance at the receiver (i.e., the AP) uses the L-LTF transmitted in the data frames.

Figure 4 allows analyzing the effects of different IQ imbalance configurations on the PER as function of SNR for MCS3 (16-QAM) over the TGac D [1,8,6,1] channel. First, assuming a PER of 1%, we can see that there is a same power loss of 7 dB for the following simulation set up: *(i)* SSB suppression of -40 dBc (with gain imbalance of 0.1875 dB and phase imbalance of 0.3º); *(ii)* the hypothetical case when there is only IQ gain mismatch of 0.1875 dB. Notice that in the above two study cases, the IQ mitigation scheme is not operational. Second, the system performance is completely degraded when there is only IQ gain impairment of 0.5 dB if any IQ mitigation scheme is implemented. Finally, notice that the proposed uplink power control and IQ gain mitigation schemes eliminate the negative effects of both different path loss (ΔP= 6 dB) among the clients and IQ impairment with only gain IQ imbalance of either 0.1875 dB or 0.5 dB. We must reemphasize that the IQ phase mitigation scheme is never operational in the simulation set up of Fig. 4.

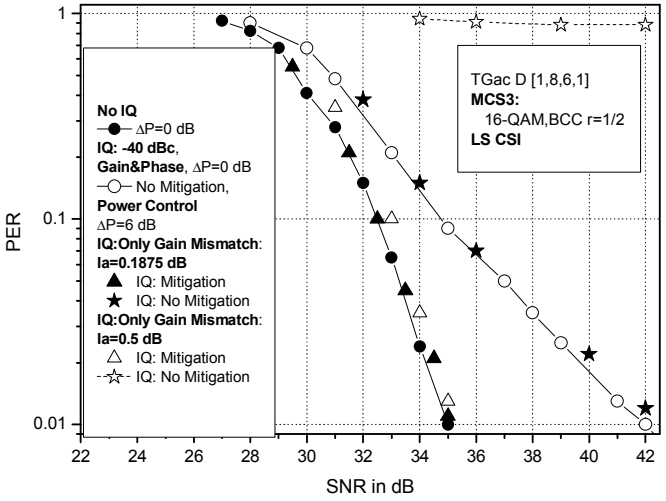

Figure 4. Effects of power control and mitigation of IQ gain imbalance on the PER: TGac D [1,8,6,1] channel; BW=80 MHz; MU-MMSE receiver with LS CSI, MPDU payload of 1500 bytes; soft-decision Viterbi decoding.

Figure 5 shows that only an IQ gain mitigation scheme is enough to mitigate the IQ imbalance in a system with SSB suppression of -40 dBc. However, Fig. 5 also depicts a performance loss of 4 dB when only the IQ amplitude mitigation scheme is operational if the SSB supression is decreased to -30 dBc, whilst it is avoided the catastropic performance degradation that happens when there is no implementation of any IQ mitigation scheme (i.e, a PER of 96% for an untangible SNR of 42 dB). Fortunatly, Fig. 5 also shows a performance loss of only 0.5 dB when both amplitude and phase are corrected using the proposed IQ imbalance estimation and correction scheme. Notice that the uplink power control scheme, described in Section IV, is operational in this simulation set up in order to counterbalance power differences of 10 dB between the stronger and weaker clients.

D. Asynchronous Uplink OFDM MU-MIMO Channel

The legacy short training field (L-STF) is the first field transmitted in the legacy preamble specified in the IEEE 802.11a/g/n/ac/ax amendments [13]. First, the L-STF is used to

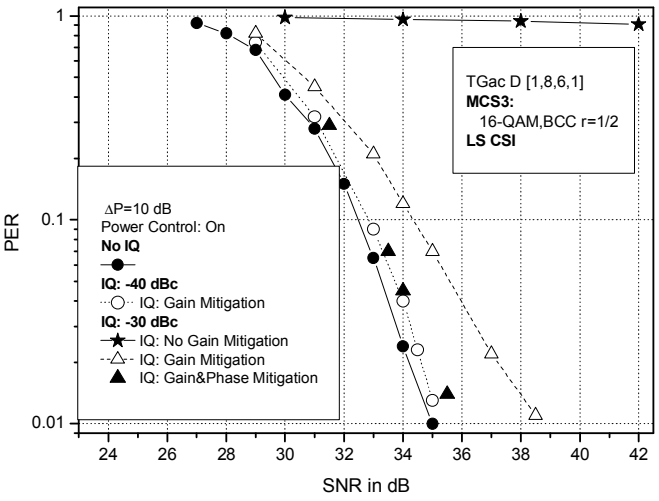

Figure 5. Effects of power control and mitigation of IQ gain and phase imbalance on the PER: TGac D [1,8,6,1] channel; BW=80 MHz; MU-MMSE receiver with LS CSI, MPDU payload of 1500 bytes; soft-decision Viterbi decoding.

implement automatic gain control (AGC). In the following, the L-STF is utilized to implement temporal synchronization and coarse estimation of the CFO [11,13]. The L-STF transports 10 repetitions of a known short symbol with period $P_{L\text{-}STF}$.

The input symbols to the temporal synchronization scheme are obtained using an equal gain combining (EGC) scheme, i.e.,

$$y[n] = \sum_{j=1}^{n_r} r_j[n], \tag{12}$$

where $r_j[n]$ is the nth sample of the symbol received at jth receive antenna.

The synchronization time θ in 802.11ax WLANs can be estimated by maximizing the autocorrelation, normalized by the received power at EGG output, of the received samples with the samples delayed by the L-STF length:

$$\theta = \max_n \left(\frac{|c_n|^2}{(p_n)^2}\right) = \max_n \left(\frac{\left|\sum_{m=0}^{L-1} y_{n+m}^* \, y_{n-P_{L-STF}+m}\right|^2}{\sum_{m=0}^{L-1} |y_{n+m}|^2)^2}\right), \tag{13}$$

where the parameter L is equal to or multiple of $P_{L\text{-}STF}$ [14-15]. In this paper, we set L to 576 since 9 short symbols of the L-STF are used, where each short symbol of the L-STF has 64 samples when the BW is 80 MHz.

It is well-known that the inaccuracies in the estimated synchronization time can originate both inter-carrier interference (ICI) and inter-symbol interference (ISI) since the discrete Fourier Transform (DFT) window range for mth OFDM symbol can include the CP of the next OFDM symbol if the estimated synchronization time is advanced w.r.t. the beginning of the mth OFDM symbol [16, pp. 61]. Although, both ICI and ISI can be avoided if a proper sample delay $\Delta\theta$ is introduced in the estimated synchronization time, as expressed by

$$\hat{\theta} = \theta + \Delta\theta = \theta + \frac{\Delta\tau}{T_s} = \theta + \Delta\tau \cdot BW, \tag{14}$$

where the synchronization delay $\Delta\tau$ is given in seconds, and T_s is the sample interval used in the OFDM PHY. For instance, assuming a BW of 80 MHz, the sample period T_s is equal to 12.5 ns (1/BW) and, therefore, 20 samples correspond to a synchronization delay of 250 ns.

The imperfect time synchronization introduces a phase offset when the DFT is applied to the received sequence, i.e.,

$$DFT\{y[n-\hat{\theta}]\} = Y[k] \cdot e^{-i\frac{2\pi k}{N_{DFT}}\hat{\theta}} = Y[k]e^{-i\phi}, \tag{15}$$

where N_{DFT} and $Y[k]$ denote the DFT length and the symbol transmitted in the kth SC, respectively. However, if there is no ICI and ISI, then this phase offset ϕ can be mitigated using the pilot symbols transported in the L-LTF [15].

Hereafter, the asynchronous reception over UL MU-MIMO channels is modelled assuming that half of the clients have ΔT ns extra delay w.r.t. to the other half [4].

Fig. 6 shows the PER as a function of SNR for the non-delayed and delayed clients, postulating a channel delay ΔT of 400 ns, using the following UL MU-MIMO channel configurations: *(i)* canonical [1,8,6,1] (on the left-side corner); *(ii)* TGac B [1,8,6,1] (on the center); *(iii)* TGac D [1,8,6,1] (on the right-side corner). Fig. 6 also shows results when all clients' waveforms arrive synchronously ($\Delta T = 0\ ns$) at the AP. The canonical UL MU-MIMO channel is a flat fading Rayleigh with impulsive response independent and identically distributed (i.i.d) between the antennas. In this figure, it is also assumed MCS3 and synchronization delay $\Delta\tau$ of 450 ns. The results shown in this figure considers perfect UL-PC and any IQ imbalance.

First, these results show that the *non-delayed clients* have a non-negligible power loss and a power loss of 2 dB for the canonical and TGac B channels, respectively. Notice that the high synchronization delay used in this example reduces the protection against the delay spread of the channel, which explains the performance loss of 2 dB observed for the *non-delayed clients* over the TGac B channel. Second, the power loss of *delayed clients* is 9 dB for the canonical channel and completely degraded for the TGac B channel (i.e., a PER of 35% for a SNR of 36 dB). This interesting characteristic is explained as follows: assuming a synchronization delay $\Delta\tau$ of 450 ns in a channel with delay ΔT of 400 ns, then the beginning of synchronization time is always inside of the CP for the non-delayed clients. However, the power loss observed for the TGac B channel occurs due to the decreasing of CP protection against the channel delay spread since a high synchronization time delay $\Delta\tau$ is assumed in this study case. Third, there is a complete performance degradation (i.e., a PER of 80% for a SNR of 36 dB) for *both delayed and non-delayed clients* for the channel TGac D due to ICI and ISI caused by the joint effects of channel delay, high delay spread and the synchronization time delay.

E. Time Advance Scheme for the 802.1ax UL MU-MIMO PHY

In the IEEE 802.11 networks, each STA in a basic service set (BSS) have a timer synchronized with the *timing synchronization function (TSF)* of every other STA associated in the BSS managed by the AP [17, pp. 197-198].

In the 802.11ax UL MU-MIMO protocol, the TF transmitted from the AP to the STAs scheduled to the next UL MU-MIMO transmission contains a field that indicates the time advance that must be used for each client in the transmission of the next UL MU Data frame [3].

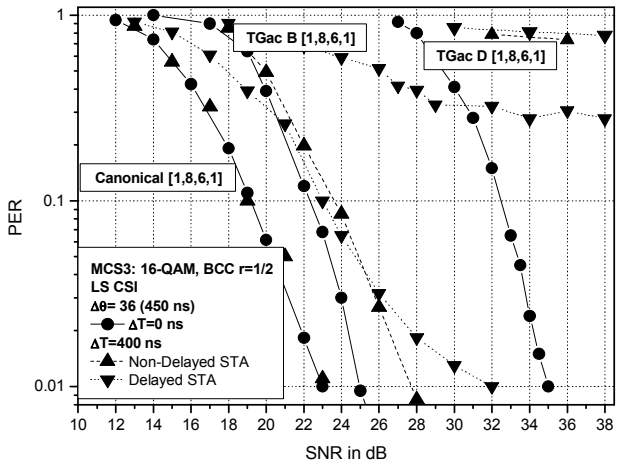

Figure 6. Comparison between the PER for delayed and non-delayed clients over canonical (on the left-side corner), TGac B (on the center), TGac D (on the right-side corner) UL MU-MIMO [1,8,1,6] channels: MCS3 (16-QAM, BCC with code rate ½); BW=80 MHz; MU-MMSE receiver with LS CSI, MPDU payload of 1500 bytes; soft-decision Viterbi decoding.

In this paper, the time advance for each client to synchronize the UL MU-MIMO channel is calculated at the AP as follows: the control frames transmitted from the clients to the AP in any single-user (SU) transmission contain the value of the TSF that informs when this control frame was transmitted. The AP estimates the received TSF using the synchronization scheme (see Eqs. 12 to 14) and its own TSF. The difference between the TSF estimated by the AP and the TSF transported in the control frame transmitted by each client is storaged in a table as an estimative of the channel delay between the client and the AP. Notice that he AP must use a SU transmission from the STAs to estimate the frame time arriving since it is not possible discriminating the arrival time of each individual client in a UL MU-MIMO transmission using (13). Finally, Fig. 7 shows that the proposed time-advance scheme allows the operation of 802.11ax UL MU-MIMO PHY over asynchronous channels.

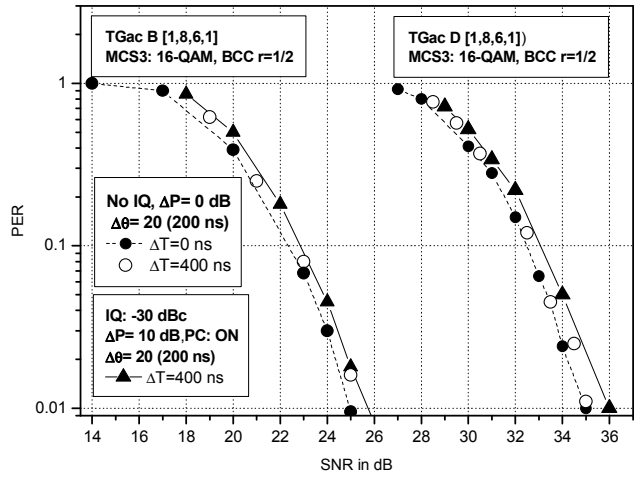

Figure 7. Comparison between the PER for a synchronous channel ($\Delta T = 0\ ns$) with the PER for an asynchronous channel ($\Delta T = 400\ ns$) when the time advance mechanism is implemented. The results for [1,8,1,6] UL-MIMO TGac B and TGac D channels are shown on the left and on the right-side corners, respectively.

VI. Conclusions

First, after developing a brief review of the current state of IEEE 802.1ax standardization process, we have described mathematical models for both phase noise (PN) and IQ imbalance hardware impairments. Second, we have developed an uplink power control (UL-PC) scheme suitable for 802.11ax PHY. Third, we have summarized the main characteristics of an IEEE 802.11ax link layer simulator. Based on the shown simulation results, we have concluded that the PN impairment below 6 GHz does not affect the system performance even when there are differences on the average received power among the clients at the AP. However, we have shown that the IQ imbalance can affect the system performance substantially. Therefore, we have implemented a joint UL-PC and time-domain IQ estimation and mitigation scheme that counterbalance the IQ impairment at both transmitter and receiver, even in environments where the clients have different path loss. Finally, after showing that the uplink asynchronous channel can degrade the 802.11ax PHY performance dramatically, we have developed and validated by simulation a time advance scheme for the 802.1ax UL MU-MIMO PHY.

References

[1] R. Stacey. *Specification Framework for TGax.* IEEE 11-15/0132r15, Jan. 2016.

[2] R. V. Nee et. al. *UL MU-MIMO for 11ac*. IEEE 802.11-09/0852-00-00ac, July 2009.

[3] R. Stacey. *Proposed TGax Draft Specification.* IEEE 802.11-16/0024r1, March 2016.

[4] R. V. Nee. *Uplink MU-MIMO sensitivity to power differences and synchronization errors*. IEEE 802.11-09/1036-00-00ac, Sept. 2009.

[5] K. Oteri and R. Yang. *Power Control for Multi-User Transmission in 802.11ax*. IEEE 802.11-16/0331r1, March 2016.

[6] A. Bharadwaj et. al. *Power Control for UL MU*. IEEE 802.11-16/0413r0, March 2016.

[7] R. Porot et. al. *11ax Evaluation Methodology.* IEEE 802.11-14/ 0571r12, Jan. 2016.

[8] M. Windisch and G. Fettweis, "Performance degradation due to I/Q imbalance in multi-carrier direct conversion receivers: a theoretical analysis," *in IEEE International Conference on Communications 2006 (ICC'06)*, 2006.

[9] I. Held, O. Klein, A. Chen and V. Ma. "Low complexity digital IQ imbalance correction in OFDM WLAN receivers," *in IEEE Vehicular Technology Conf.*, vol. 2, pp. 1172-1176, May 2004.

[10] E. Nash, "Correcting imperfections in IQ modulators to improve RF signal fidelity," in *Analog Devices, Application Note AN-1039***.**

[11] R. P. F. Hoefel. "IEEE 802.11ax: A study on techniques to mitigate the frequency offset in the uplink multi-user MIMO", in *8th 2016 IEEE Latin-American Conference on Communication (LATINCOM 2016),* Medellin, Colombia, Nov. 2016.

[12] S. Veramani and A. V. Zelst, *Interference Cancellation for Downlink MU-MIMO*. IEEE 802.11-09/1234r1, 2010.

[13] E. Perahia and R. Stacey, *Next Generation Wireless LANS*: *802.11n and 802.11ac.2th ed*. Cambridge: Cambridge University Press, 2013.

[14] R. Spitschka, *Synchronization Algorithms for OFDM Systems Using the Example of WLAN*. Saarbrucken, Germany: VDM Verlag, 2008.

[15] R. P. F. Hoefel. "On the synchronization of IEEE 802.11n devices over frequency selective TGn channel models," *25th Annual Canadian Conference on Electrical and Computer Engineering (CCECE 2012),* Montreal, 2012.

[16] J. Heiskala and J. Terry, *OFDM Wireless LANs: A Theoretical and Practical Guide.* Indiana: SAMS Publishing, 2001.

[17] M. S. Gast, *802.11 Wireless Networks*. Boston: O'Reilly, 2005.